

Instructions: The response to the Referees shall be structured in a clear and easy to follow sequence: (1) comments from Referees, (2) author's response, (3) author's changes in the manuscript. (Note on spectral DOI's is on p.7). In addition, please provide a marked-up manuscript version showing the changes made (using track changes in Word or latexdiff in LaTeX). This version should be combined with your response file so that the Editor can clearly identify what changes have been made. (Note: track changes in Word begins on page 8).

(1) comments from Referees

RC1:

General comments

10 Balazs et al. present an addition to their NAMFIS approach which now includes characterization of populations of alternate conformations and dynamics of the molecules under study. With the replica exchange approach, simulations times are virtually extended such that slow conformational exchanges can be accessed. The refined approach supports prospective ranking of design ideas in medicinal chemistry in a very efficient manner and sheds light onto alternative conformations and dynamics. Further, REST-MD indicates where potentially
15 interesting alternate conformations and dynamics may occur which should be tested by NMR experiments, thereby much simplifying and reducing the NMR analysis in a targeted manner.

Specific comments

Why were NMR experiments carried out in DMSO? This is somewhat puzzling since the MD simulations were carried out in explicit water with NaCl. I could well imagine that alternative conformations are populated
20 differently in DMSO than in aqueous buffer. Also, activity assays used to identify the bioactive conformation are carried out in aqueous buffer.

The MD protocol seems to yield very nice results for those torsion angles with an energy barrier < 10 kcal/mol. However, there are some questions about the rotation with the 25 kcal/mol barrier in the top right diagram in Figure 3b: Why aren't the two rotational energy barriers of identical height? The one at -170° seems to agree
25 with the experimental value, while the one at 10° seems significantly higher.

Figure 3b, top right diagram: the profile seems to imply lower energy for the +100° rotation angle, yet the populations are opposite.

The molecule presented is a very nice example of hindered rotation. However, it would be very instructive in order to assess the method, if more than just one example would be shown. But I guess that this is not possible
30 due to trade secrets.

In order to reproduce such simulations, what would be your recommendation for the maximal temperature of the simulation? 3300 K looks a bit harsh, but seems to be required to compensate for short simulation times, even with replica exchange.

35 For prioritization of design ideas, relative populations of alternative conformations are important. The populations in Figure 5 however don't seem to correlate with the actual populations observed by NMR. In your experience, which parameter of the simulation should be used to derive relative populations? Populations during MD (blue histograms), fragment based energy landscape (solid blue lines) or a combination of these parameters?

40 A very similar question comes up for how the dynamics in the MD correlate with the NMR experiment: Should the calculated energy barrier of rotation be used or how often an alternate conformation was visited in the MD?

45 Could references be provided that support the statements that NMR provides information on permeability and bioavailability etc.?

RC2:

50 In the present manuscript Chiarparin and coworkers describe the use of the REST-MD method (replica exchange with solute tempering in explicit water, introduced by the Friesner and Bern groups in 2005) as a means to investigate the conformational preference of small molecules in order to inform drug design. While I believe that this manuscript presents solid science that would be publishable in principle (subject to minor revisions), I cannot see that it fits within the scope of Magnetic Resonance, because it does not present any advancements related to NMR. The manuscript describes a very brief case study that nicely illustrates the utility of REST-MD and the fact that NMR experiments can provide corrective results that augment the full picture during the drug design process. However, the use of NMR is limited to standard techniques to determine the rotamer populations and the rotamer barrier of a single torsion in a pair of congeneric molecules, as a means to validate results from REST-MD. In part, the manuscript reads like a review of what has been (or could be) performed in other studies in terms of using NMR data to guide REST-MD calculations and other computational approaches. It is not at all clear what is actually new in this manuscript, except the specific results for this particular set of molecules.

60 I would suggest that the authors expand the scope of the manuscript by incorporating a larger set of NMR data, as the authors also suggest on p. 8, and clearly show how such data can be used to curate results from REST-MD calculations, or possibly introduce NMR-based constraints to guide calculations so as to truly make the calculations 'interpret' the NMR data. At present, the manuscript merely presents a brief (but nice) illustration of the use of REST-MD, followed by validation by NMR.

65 Minor points:

The REST-MD simulations involve explicit water, whereas the NMR studies used DMSO as solvent. Please comment on whether you expect deviations in rotamer populations due to the different solvents. Is it not possible to perform the NMR studies in water?

Fig. 2: Please highlight the benzylic CH group in the chemical structures to the left.

70 Fig. 2: Please define logD, as a service to readers outside of the medicinal chemistry field.

line 197-198: "...designing an increase in the percent bioactive conformation by restricting rotation". This sentence apparently confuses kinetics/dynamics with thermodynamics. Rotation is restricted by changing the barrier height, but this does not necessarily affect the relative populations of the two rotamer states, unless one of the two states is preferentially stabilized over the other, in which case it suffices to state just that, leaving the barrier (or restriction of rotation) out of the picture. There is similarly imprecise wording on lines 35-36.
75

line 207-210. I do not understand this sentence, please consider rephrasing. What is "low mode MD...?"

(2) author's response

Reply on RC1:

Q: Why were NMR experiments carried out in DMSO? This is somewhat puzzling since the MD simulations were carried out in explicit water with NaCl. I could well imagine that alternative conformations are populated differently in DMSO than in aqueous buffer. Also, activity assays used to identify the bioactive conformation are carried out in aqueous buffer.
80

A: In our experience with small molecule drug candidates, in DMSO the conformer populations reproduce well those in buffer (pH 7); (for example: <https://doi.org/10.1021/acs.jmedchem.9b00716>). Therefore, we use DMSO in routine application of this approach to ensure consistency across ligands, since solubility issues will often arise in pure water. This combination of water models with DMSO-derived data reflects the actual medicinal chemistry workflow.
85

Q: The MD protocol seems to yield very nice results for those torsion angles with an energy barrier < 10 kcal/mol. However, there are some questions about the rotation with the 25 kcal/mol barrier in the top right diagram in Figure 3b: Why aren't the two rotational energy barriers of identical height? The one at -170° seems to agree with the experimental value, while the one at 10° seems significantly higher.
90

A: High rotational barriers will be subject to hysteresis and sampling effects and it is not possible to assign rigorous values to those barriers. The profiles are indicative of barrier height, but we rely on NMR data to rationalize these.

Q: Figure 3b, top right diagram: the profile seems to imply lower energy for the +100° rotation angle, yet the populations are opposite.
95

A: The minima lie at the same energy but sampling has been limited, as discussed further in Fig 5.

100 Q: **The molecule presented is a very nice example of hindered rotation.** However, it would be very instructive in order to assess the method, if more than just one example would be shown. But I guess that this is not possible due to trade secrets.

A: (Thanks!) Yes, the matched pair exemplar supports the complementarity of the computation and experiment for use as a platform to guide design, while keeping within the highest practicality for our current scope.

105 Q: In order to reproduce such simulations, what would be your recommendation for the maximal temperature of the simulation? 3300 K looks a bit harsh, but seems to be required to compensate for short simulation times, even with replica exchange.

110 *A: In REST-MD the temperature is only a surrogate value, since the Hamiltonian is actually modified rather than the temperature. Other groups use the terminology Hamiltonian replica exchange to distinguish this from standard temperature replica exchange. We show this very high surrogate temperature to demonstrate that sampling of high torsional barriers can be limited, even when the Hamiltonian is modified to mimic such a high temperature.*

115 Q: For prioritization of design ideas, relative populations of alternative conformations are important. The populations in Figure 5 however don't seem to correlate with the actual populations observed by NMR. In your experience, which parameter of the simulation should be used to derive relative populations? Populations during MD (blue histograms), fragment based energy landscape (solid blue lines) or a combination of these parameters?

A: In a case where we see no issues with sampling of hindered rotations, as discussed in Fig 5, we use Boltzmann counting to assign simulation populations, after clustering using full-molecule RMSD. This would correspond to the circular histograms.

120 Q: A very similar question comes up for how the dynamics in the MD correlate with the NMR experiment: Should the calculated energy barrier of rotation be used or how often an alternate conformation was visited in the MD?

125 *A: In principle the MD trajectory should equilibrate to Boltzmann-weighted populations, consistent with the free energy of each conformational state. We use the computed torsion barriers to guide analysis of NMR data and look for consistency between barrier heights and NMR signals. As noted above, it is not guaranteed that an unbiased MD trajectory will be able to explore all the conformers and cross all barriers to establish an equilibrium population. The most effective approach that we have found is to look at both experimental and computational data and to rely on models only when we have robust evidence that we are seeing trends consistent with experiment.*

130 Q: Could references be provided that support the statements that NMR provides information on permeability and bioavailability etc.?

ie: p.12 lines 288-289: In addition, NMR provides design teams with information on the presence of intramolecular hydrogen bonds (IMHB), and the combined influences on properties such as potency, permeability and oral bioavailability

A: (1) Alex, A., et al., *Med. Chem. Commun.*, 2011, 2, 669-674, <https://doi.org/10.1039/C1MD00093D>

135 (2) Over, B., et al., *Nat Chem Biol.*, 2016, 12, 1065-1074, doi: 10.1038/nchembio.2203.

Reply on RC2:

Q: Expansion of scope

140 *A: While NAMFIS and related methods provide conformer populations, the energy barriers and rotational dynamics are typically not quantified, despite being available from the NMR signal linewidth. This manuscript quantitatively compares for the first time, using a rotameric drug-like exemplar, measurements of both conformer populations and rotational dynamics with in silico calculated values. As discussed in section 2.4 on synergy of methods, our novel implementation of these tools are advancing the current state of the art in performing semi-automated structure and dynamics (the latter often underutilized) analyses of a free ligand in a drug discovery setting, including prospective molecular information, to guide drug design.*

145

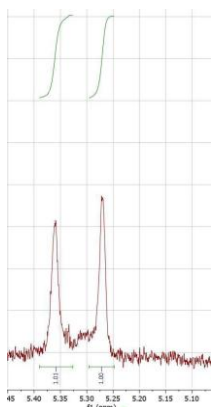
Q: introduction of NMR based restraints to simulations

150 *A: While using NMR data to guide computational MD approaches is well established, it would not be prospective. Line 201 discusses the added benefit of delivering prospective information on molecules not yet synthesized. In a Design-Test cycle, for an exemplar of a chemical series of analogs experimental data is generated. This is used to evaluate the limitations of the in silico data sufficiently well to confidently rank order design ideas and select which to progress on to real world, resource intensive, syntheses.*

Q: Expect solvent effects on rotamers populations between DMSO and water?

155 *A: We might expect population differences between apolar and polar solvent (<https://pubs.acs.org/doi/pdf/10.1021/ja042890e>). However, in our experience with small molecule drug candidates, in DMSO the conformer populations reproduce well those in buffer (pH 7); (for example, <https://doi.org/10.1021/acs.jmedchem.9b00716>). We would not expect significantly different rotamer populations between DMSO and water in this molecule. An intramolecular energy barrier >20 kcal/mol should not depend on the solvent, population differences would not be expected in our experience.*

160 *Experimentally, compound (2) gives 1:1 rotamers when acquired in CDCl₃ (below) and is insoluble in buffer, pH 7.*



Q: Is it not possible to perform the NMR studies in water?

A: We believe DMSO is the most tractable option for this type of experimental platform. In consideration that the populations between DMSO and water are expected to be quite similar, and especially in consideration that aqueous solubility is often quite low for small molecule candidate drugs, DMSO- d_6 provides a consistent and pragmatic solution (<https://doi.org/10.1021/acs.jmedchem.9b00716>).

165

Request: Fig. 2: Please highlight the benzylic CH group in the chemical structures to the left.

Response: In the uploaded revised version: a star was added to the structures in Figure 2, and in line 91, "(the starred CH in ring 'C')"

170 Request: Fig. 2: Please define logD, as a service to readers outside of the medicinal chemistry field.

Response: Added to the Figure 1 caption, line 49-50, "with inhibition (pIC_{50}) and the octanol/water partition coefficient (logD) values from a recent Oncology R&D project (Scott et al., 2016; Scott et al., 2019; Scott et al., 2020)" to clarify the first occurrences of the binding parameter, pIC_{50} , and the partition coefficient, logD.

Comment: line 197-198: "...designing an increase in the percent bioactive conformation by restricting rotation".

175 This sentence apparently confuses kinetics/dynamics with thermodynamics. Rotation is restricted by changing the barrier height, but this does not necessarily affect the relative populations of the two rotamer states, unless one of the two states is preferentially stabilized over the other, in which case it suffices to state just that, leaving the barrier (or restriction of rotation) out of the picture.

Response: Yes, thank you, this is about thermodynamics. To help clarify, the new line in the uploaded manuscript is, "...of design team effort invested in increasing the percentage of free ligand pre-organized into a bioactive conformation." This should help distinguish that "design" refers to creation of a new molecule with increased population of bioactive conformation.

180

Comment: There is similarly imprecise wording on lines 35-36.

*Response: updated sentence, added the words in bold (not bolded in the manuscript) "...the challenge is to conceive of ideas to modify the **structure to discover a new** molecule that favors the bioactive conformation."*

185

Comment: line 207-210. I do not understand this sentence, please consider rephrasing. What is "low mode MD..."?

Response: line 207-210, after "low mode MD..." reference added in line: (LaBute, 2010) and to reference list:

Labute, P.: LowModeMD-Implicit Low-Mode Velocity Filtering Applied to Conformational Search of Macrocycles and Protein Loops, *J. Chem. Inf. Model.*, **50**, 792-800, <https://doi.org/10.1021/ci900508k>, 2010.

190

(3) author's changes in the manuscript

- lines 35-36, added clarifying phrase to the sentence, "...the challenge is to conceive of ideas to modify the **structure to discover a new** molecule that favors the bioactive conformation."
- Figure 1 caption, line 49-50, "with inhibition (pIC_{50}) and the octanol/water partition coefficient ($\log D$) values from a recent Oncology R&D project (Scott et al., 2016; Scott et al., 2019; Scott et al., 2020)" to clarify the first occurrences of the binding parameter, pIC_{50} , and the partition coefficient, $\log D$.
- Figure 2, a star was added to the structures, and line 91, "(the starred CH in ring 'C') was added for clarity in the figure caption.
- Line 198, to help clarify, the new line in the uploaded manuscript is, "...of design team effort invested in increasing the percentage of free ligand pre-organized into a bioactive conformation."
- From Line 208, the following is the updated text, "Using the conformer set generated by REST-MD is particularly helpful for higher molecular weight small molecules which begin to self-associate during low mode MD conformational searches (LaBute, 2010) using a polarizable continuum model to emulate solvent. Low mode MD provides a comprehensive search of the conformational ensemble, but can therefore result in a set highly biased towards collapsed conformations."
- Line 367, reference list, alphabetically added reference: Labute, P.:

195

200

205

210 **(4) Chemotion DOI's**, for 1D 1H NMR spectral database submissions (will work only after release of the embargo post-publication, <https://www.chemotion.net/>):

<https://dx.doi.org/10.14272/WCXZZJFDRDQAHJ-WXTAPIANSA-N.1>

<https://dx.doi.org/10.14272/GRTREOMLNXYRCK-CRICUBBOSA-N.1>

<https://dx.doi.org/10.14272/UZTVFIJYDQIRSV-MZNIJEOGPSA-N.1>

NMR free ligand conformations and atomic resolution dynamics

Amber Y.S. Balazs¹, Nichola L. Davies², David Longmire², Martin J. Packer², Elisabetta Chiarparin²

¹Chemistry, Oncology R&D, AstraZeneca, Waltham, Massachusetts 02451, United States

²Chemistry, Oncology R&D, AstraZeneca, Cambridge CB4 0QA, United Kingdom

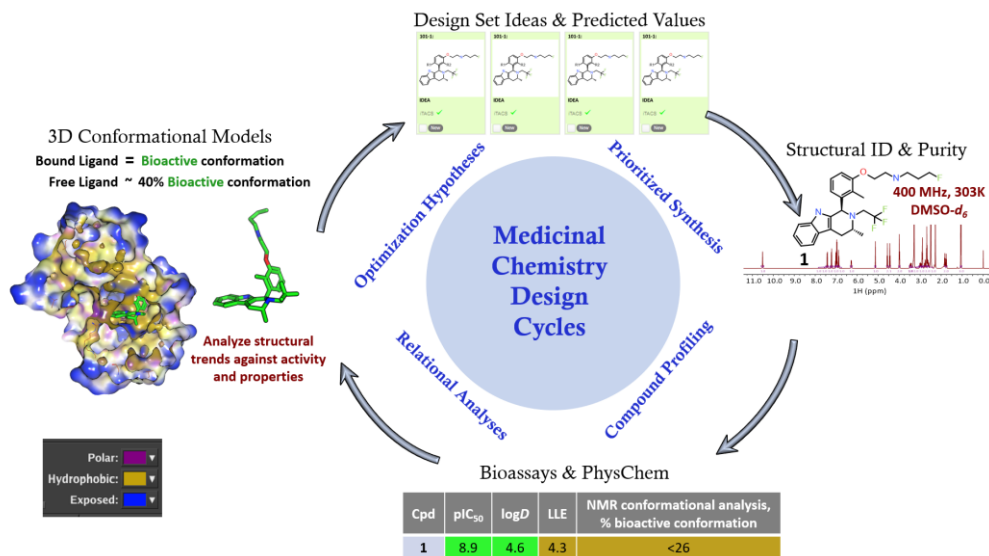
5 *Correspondence to:* Amber Y.S. Balazs (amber.balazs@astrazeneca.com)

Abstract. Knowledge of free ligand conformational preferences (energy minima) and conformational dynamics (rotational energy barriers) of small molecules in solution can guide drug design hypotheses and help rank ideas to bias syntheses towards more active compounds. Visualization of conformational exchange dynamics around torsion angles, by replica-exchange with solute tempering molecular dynamics (REST-MD), gives results in agreement with high resolution ¹H NMR spectra and complements free ligand conformational analyses. Rotational energy barriers around individual bonds are comparable between calculated and experimental values, making the *in silico* method relevant to ranking prospective design ideas in drug discovery programs, particularly across a series of analogues. Prioritizing design ideas, based on calculations and analysis of measurements across a series, efficiently guides rational discovery towards the 'right molecules' for effective medicines.

15 1 Introduction

NMR signal line shapes inherently provide atomic-level, site-specific insights into structural dynamics. High resolution ¹H NMR signals broaden when small molecules in solution undergo exchange dynamics on a millisecond timescale. In contrast, sharp NMR resonance signals may indicate either a dominant pre-organized conformation or an ensemble of flexible molecules undergoing fast equilibrium exchange between rotational isomers. Comparisons between experimental and computed NMR parameter values (shifts, NOEs, *J*-couplings) can identify relative populations of conformers, such as a singular, highly populated conformation, with well defined internuclear distances and torsion angles or an averaged solution structure, composed of multiple conformations, each at a low molar fraction of the total, resulting from low barriers to rotation around bonds. NMR analysis of molecular flexibility in solution (NAMFIS; Cicero et al., 1995) takes the approach of systematically varying percent contributions from sets of conformers generated *in silico*, together with the corresponding *calculated* NMR parameter values, compared against the experimental data. The sum of square differences determines the goodness-of-fit between experimental and calculated values to select a best-fit population weighted model. The fundamental concept of filtering theoretical conformations through experimental data to derive the best fit has become well established over the decades, together with variations in details of implementation, to determine the conformational preference(s) of a small molecule in solution (Cicero et al., 1995; Nevins et al, 1999; Slabber et al., 2016; Wu et al., 2017; Balazs et al., 2019; Farès et al., 2019; Atilaw et al., 2021).

Determining the conformational profile of a free ligand in solution enhances early drug discovery programs (LaPlante et al., 2014; Blundell et al., 2016; Foloppe and Chen, 2016; Chiarparin et al., 2019). A general overview of how NMR fits into Medicinal Chemistry design cycles is illustrated in Fig. 1. An efficacious pharmaceutical that positively impacts patients' lives starts with Medicinal Chemistry teams designing the right molecule. Design teams need to understand whether a molecule readily adopts its "bioactive" conformation in solution to optimize the binding on-rate through reduced conformational entropy and energetic penalty paid on conformational rearrangement to the proper binding mode. In addition, pre-organization of the free ligand in solution would indicate minimized conformational strain energy in the bound molecule. If not, the challenge is to conceive of ideas to modify the structure to discover a new molecule to favor this conformation. Towards this aim of optimizing the free energy of binding, it is desirable for ligands in solution to preferentially pre-organize into the bioactive binding mode (Blundell et al., 2013; Balazs et al., 2019). Molecular rigidification strategies (Fang et al., 2014; de Sena M Pinheiro et al., 2019) increase pre-organization and NMR conformational analysis can deconvolute and report on the molar fraction adopting the bioactive conformation. Structure based drug design (SBDD) can be enhanced by ready access to 3D free ligand average solution conformations to complement X-ray crystallographic models of the bound ligand and protein-ligand interactions (Blundell et al., 2013; Chiarparin et al., 2019; Balazs et al., 2019). Faster design cycles require quick turnover times in analyzing solution conformations of synthesized compounds. Design cycles can be accelerated through faster computational schemes, efficient automation to obtain NMR spectral parameters, and recognition of conformational signatures from 1D NMR spectra (Balazs et al., 2019), also named, "SAR by 1D NMR" (Zondlo, 2019).



50 **Figure 1. An illustrative Medicinal Chemistry design cycle for drug discovery with inhibition (pIC_{50}) and the octanol/water**
partition coefficient ($\log D$) values from a recent Oncology R&D project (Scott et al., 2016; Scott et al., 2019; Scott et al., 2020).
NMR plays a key role in synthesis support for structural identification and analysis of compound purity. NMR also can be used to
enhance structure based drug design through NMR free ligand conformational analysis. This provides the relative population of
the bioactive conformation in solution by determining the percentages of the minimal energy conformers. Structure based drug
design is enhanced through measured extent of free-ligand pre-organization into the bioactive conformation, which lends itself to
55 **rigidification design hypotheses aimed at optimized binding to the protein target.**

Herein, we demonstrate incorporation of molecular dynamics, specifically an efficient version using replica-exchange with
solute tempering (REST-MD) (Liu et al., 2005; Huang et al., 2007; Wang et al., 2011), into an NMR based semi-automatic
drug discovery platform, to visualize rotational barriers around molecular bonds. Good agreement is demonstrated between
REST-MD calculated energy barriers and NMR measurements, using a small molecule selective estrogen-receptor degrader
60 (SERD) example from a recent Oncology R&D project (Scott et al., 2016; Scott et al., 2019; Scott et al., 2020). The
theoretical and experimental data complement each other: REST-MD simplifies the interpretation of NMR conformational
dynamics, while the experimental NMR results can inform calculations by defining site-specific preferred torsions of the
dominant conformer and experimental conformer distributions, which may influence the initial REST-MD 3D geometry and
the sampling ergodicity achieved, as reflected in the resultant histograms.

65 **2 Results and Discussion**

2.1 NAMFIS plus NMR line shape analysis

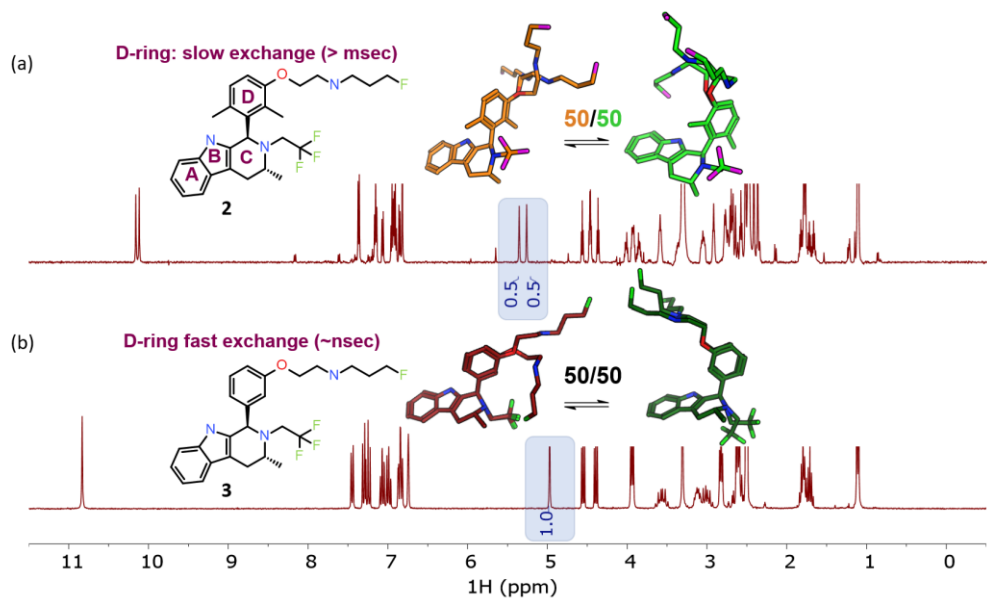
The ability of NMR to provide information on conformational dynamics, in addition to giving information on
conformational preference, is useful in small molecule drug discovery. In Fig. 2a, each peak is doubled for compound **2** (1:1
ratio), instantly recognizable to NMR users as slow exchange of rotamers due to hindered bond rotation (measured half-life ~
70 0.5 sec). As a guide to the eye, the signal(s) for the benzylic CH proton at ~ 5 ppm is/are highlighted in Fig. 2. The NMR
spectrum reports two dominant conformers, equally populated, for the free ligand in solution for compound **2**. The bioactive
conformation is one of a family of conformers (shown in green) with some flexibility around the pendant base. The
alternative conformation (shown in orange) is the other, giving ~ 50% of the compound locked in a non-bioactive
conformation. In contrast, Fig. 2b shows that compound **3** has a single set of sharp signals due to fast exchange (corresponds
75 to a typical half-life of ~ nanoseconds, $\Delta\nu_{1/2} = 2.8$ Hz). The ^1H NMR spectrum has a single isotropic chemical shift for both of
the protons within one CH_2 functional group (these are not diastereotopic), an indication of local flexibility quickly picked
up by an edited ^{13}C HSQC spectrum. Appreciation of the temporal dependence of free ligand exchange dynamics on NMR
spectra can quickly inform medicinal chemists on local flexibility around bonds of newly synthesized molecules. This
analysis, combined with potency data and matched molecular pair analysis, or a full comparison across a congeneric series,
80 can provide critical insights into structure-activity relationships (Balazs et al., 2019).

Together with information regarding relative populations of conformations in solution, information about the magnitude of
the rotational energy barrier between conformations, i.e. between one rotational isomer and another, is relevant information.

Formatted: Subscript

Formatted: Font: Italic

85 The challenge has been to get quick, easy, and comprehensive, yet accurate torsional profiles. Building a practicable and prospective visualization of conformational exchange dynamics around torsion angles into an NMR conformational analysis platform increases the potential to impact design, by highlighting the potential energy penalty of restricting torsions. To evaluate the dynamics, incorporating REST-MD into the workflow met the goal of expanding the current free ligand conformational analysis platform to make use of kinetic parameters from NMR spectra, e.g. signal line widths, while keeping within practical time limit constraints for Medicinal Chemistry design cycles.



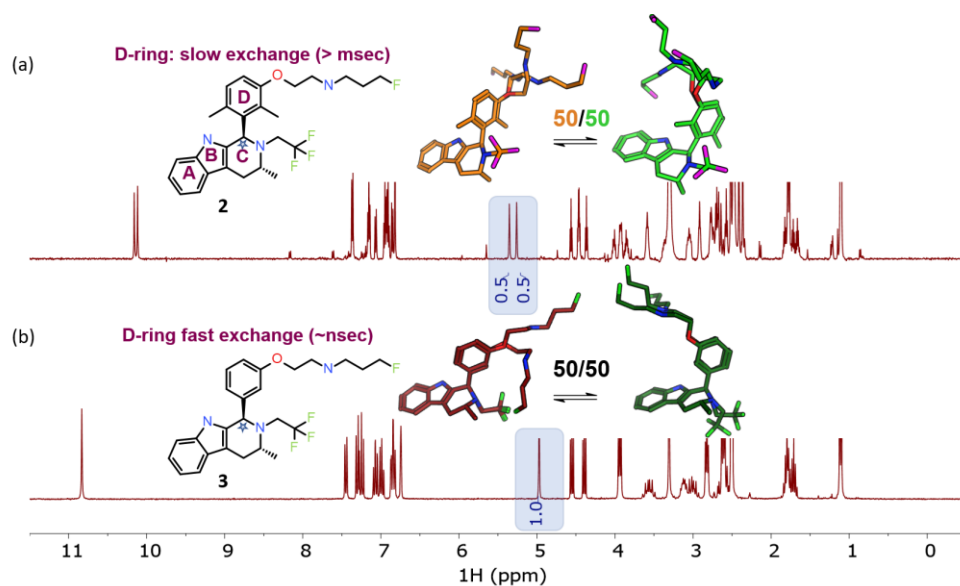
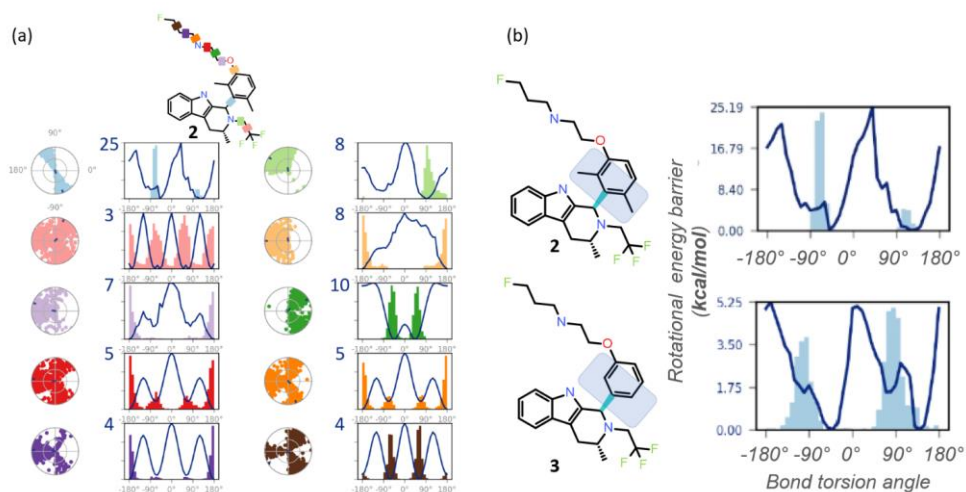


Figure 2 . NMR spectra inherently capture kinetic information from conformational dynamics (rotational energy barriers) in the signal line widths. The benzylic CH (the starred CH in ring 'C') is highlighted to exemplify the spectral changes between the dimethyl and des-methyl analogs. (a) The ¹H NMR spectrum shows rotamers with equal populations undergoing slow exchange on the NMR timescale. Profiling of 2 gave pIC₅₀ 8.9 and logD 4.8, with 50% bioactive conformation of the free ligand in DMSO-*d*₆ solution. (b) A spectrum with population weighted conformational averaging due to low barriers to rotation around bonds and fast exchange on the NMR timescale. Profiling of 3 resulted in pIC₅₀ 8.8, logD 4.1, 50% free ligand solution bioactive conformation. For this molecular matched pair we see similarities in the percent bioactive conformation in solution and the potency, regardless of the increased logD.

REST-MD predicts a comprehensive torsional profile in silico for rotatable bonds represented in a 2D molecular structure, while keeping computational speed and accuracy high. GPUs make REST-MD calculations feasible within drug discovery design cycle times. Ligand-based REST-MD simulates a ligand in explicit solvent at room temperature, allowing for conformational effects often neglected due to computational expense. The ligand conformers are sampled according to their Boltzmann populations and resultant reports visualize rotational torsion energies (Fig. 3). High accuracy fragment based calculations of rotational energy barriers (kcal/mol) are plotted as a function of bond torsion angle (solid lines). A superimposition of histograms counting the number of times the particular bond was observed at any particular angle is plotted onto the rotational energy barrier plot showing the torsion potential at each dihedral angle, summarizing the conformational space sampled during the REST-MD simulation. Such reports augment the ¹H NMR spectral interpretation, providing quantitative energy minima and theoretical distributions of conformers.



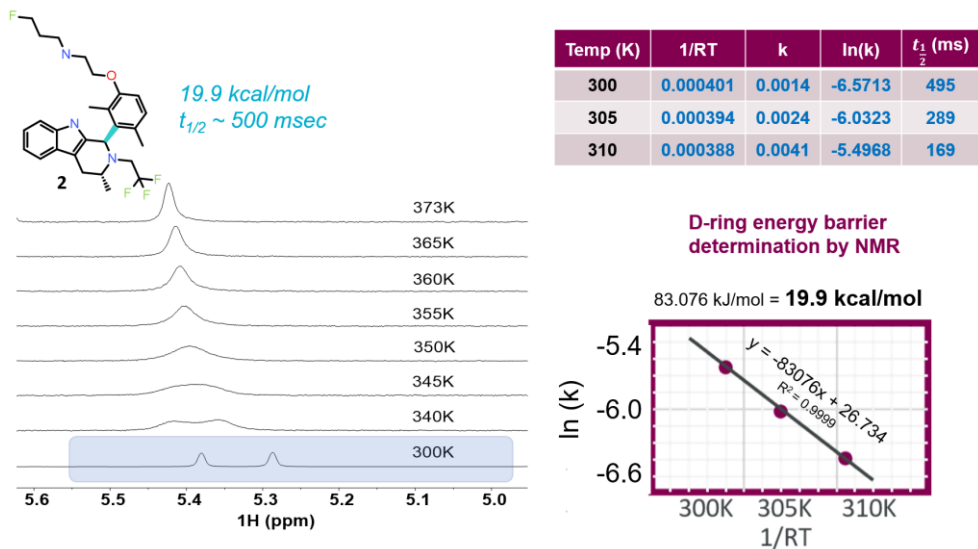
110 Figure 3. REST-MD visualizations, implemented in Maestro (Schrödinger, 2020b) complement atomic resolution NMR
 115 interpretations of structural dynamics across all bonds. (a) Simulation interaction diagrams report the rotational energy barrier
 (kcal/mol) as a function of the bond rotation angle. The conformational space sampled during the simulation is reported either as a
 function of the simulation time (radial plots, from the center at the start and spiraling outward) or as histograms superimposed on
 the torsion energy profiles (kcal/mol vs bond angle across each color coded bond in the molecule). Profiles are readily compared
 between molecular bonds that are pre-organized (light blue with y-axis maximum in the plot at 25 kcal/mol, with a bimodal radial
 120 plot and two energy minima), and flexible (pink with 3 kcal/mol maximum y-axis value, three energy minima, equally populated,
 and a randomly populated radial plot). (b) The barrier to rotation of the dimethyl is calculated to be, based on the lower of the two
 barriers, ~20 kcal/mol. Whereas experimentally both energy minima are equally populated as seen by the 1:1 ratio by NMR,
 the sampling conditions of the rigid “blue” bond were insufficient in the simulation to equally populate both wells. The NMR data in
 such cases clearly informs on the calculated predictions. A separate REST-MD simulation for the des-methyl compound, 3, was < 6
 125 kcal/mol calculated rotational energy barrier for the same “blue” bond, consistent with sharp lines and ready conversions between
 the two conformers, with a broadened range of torsions, albeit still bimodal.

2.2 NMR measured rotational energy barrier

Methylation is a familiar and fundamental structural rigidification tool in a Medicinal Chemist’s toolbox. In Fig. 2
 125 methylation of the D ring demonstrates restricted bond rotation by the presence of rotameric signals in the ¹H NMR
 spectrum. Such restricted bond rotations, on millisecond timescales, occur when barriers to rotation about a bond are high
 (>~15 kcal/mol under ambient conditions). In contrast, a structural analog without methyl groups on the D ring displays free
 bond rotation on the NMR timescale (~ nanoseconds). Typically such barriers to rotation at room temperature correspond to
 ~ 5 kcal/mol (LaPlante et al., 2011a; LaPlante et al., 2011b; Wipf et al., 2015). The NMR spectrum of the ensemble of
 130 rapidly exchanging conformations reflects the Boltzmann weighted average of the chemical shifts, *J*-couplings, and
 interproton distances, with a single set of sharp peaks.

To locate the bond with the hindered rotation, chemical intuition is often sufficient. Using variable temperature NMR and/or exchange spectroscopy, the rotational energy barrier and the torsional rotation half-life of exchange can be determined. Fig. 4 shows ^1H NMR spectra as a function of eight different temperatures. The spectrum near room temperature has two equal rotameric populations undergoing slow exchange on the NMR timescale, and highlighted in the figure. With increasing temperature the peaks coalesce and then begin to narrow. Increasing the temperature not only increases the rotation rate of the aromatic ring, it also increases the rate of fluctuations in the pendant base and the CH_2CF_3 groups and between axial vs. equatorial methyl orientation in ring C. Overall, this drives a shift to higher ppm for the exchange averaged signal with increasing temperature (Fig. 4).

135



140

Figure 4. VT NMR stacked plots for the dimethyl compound undergoing slow to fast exchange with increasing temperature. To measure the energy barrier to rotation of the D-ring, three temperatures and a 1D selective EXSY at different mixing times was used to estimate the exchange rates and half-life. An Arrhenius plot gives the barrier to rotation at 19.9 kcal/mol and the 300 K half-life is ~ 0.5 sec.

145

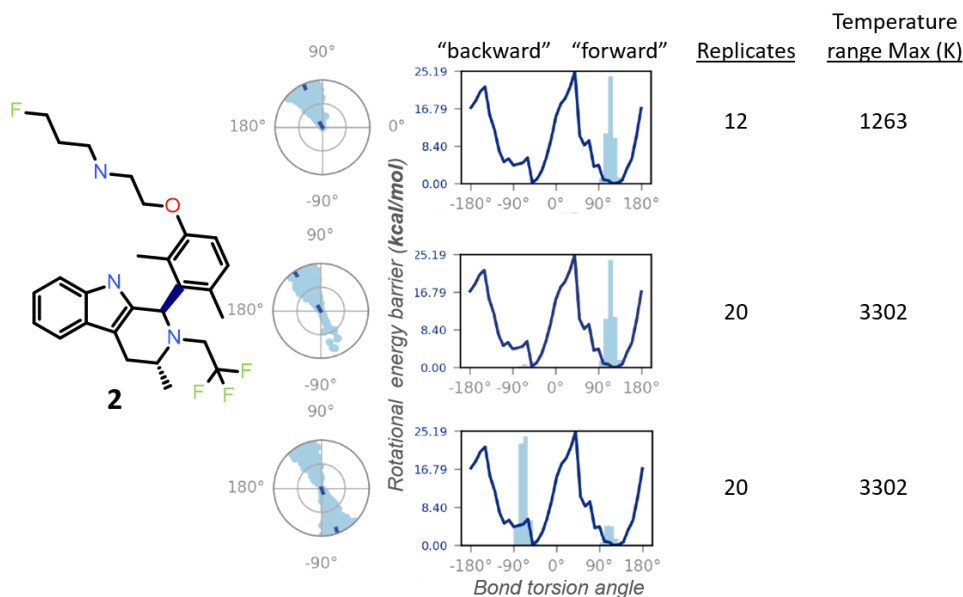
In order to determine the barrier to rotation around the aromatic ring, it was important to collect data within a temperature range where exchange rates were dominated by the dynamics of interest in order to follow a simple two-state model for analysis. Therefore, three temperatures at 300, 305, and 310 K were chosen and exchange spectroscopy was performed with selective inversion on the peak near 5.3 ppm. At each of the three temperatures 8 mixing times (100, 200, 300, 400, 500, 700, 1000, and 2000 milliseconds) were used to determine the first order rate kinetics, with the fitted value for k given in

150 tabular form in Fig. 4. The half-life was derived from $\ln(2)/k$. The fitted plot of $\ln(k)$ vs. $1/RT$ is shown, revealing a value of
19.9 kcal/mol for the barrier to rotation.

2.3 NMR informs calculations

REST-MD generates a large ensemble of (~1000) conformations, in explicit solvent. REST-MD was run with Desmond
(Schrödinger, 2020a) with the pendant base initially oriented either forward or backward relative to the tricyclic core for **1**.
155 The resultant calculated energy barrier of ~ 20 kcal/mol (Fig. 3b) is in agreement with the NMR determined value of 19.9
kcal/mol. The REST-MD visualization confirmed chemical intuition that the source of the rotameric species is the bond
between the tricyclic core and the aromatic ring. Advantageously, the full torsional profile report from the REST-MD
simulation can be run prospectively to rank design ideas, for instance to test a hypothesis around rigidification and the degree
of bioactive pre-organization induced. The ability of REST-MD to evaluate torsion angles prior to synthesis can also flag
160 chemists to check the NMR for site-specific dynamics information at the time of structural verification. Such information
could alert the team to add a diagnostic selective-NOE measurement to the standard acquisition suite, to test a free ligand
conformational hypothesis post synthesis, while the solution sample is in the spectrometer for structural identification.

Conversely, the NMR can supply experimental details inaccessible to the calculations, particularly helpful within a chemical
series, as the lessons are generally translatable across the structural analogs. For instance, the ^1H NMR spectrum of the
165 dimethyl compound **2** showed a 1:1 ratio between the two exchanging conformations (Fig. 2). Whereas REST-MD
conformational sampling shows only one of the two minima populated (Fig. 5). The fragment based energy calculation,
shown as a solid line in the REST-MD torsional profiles, is consistently the same, even using a very short simulation time
(e.g. picoseconds). The histograms vary based on initial conformation and number of replicates run. Starting with an initial
conformation with the pendant base facing "forward" relative to the tricyclic core, the radial plot of torsion angle
170 representation as a function of time starting at the center and spiraling outward, only populates the ~ +90° bond torsion angle
during the 50 ns simulation that has a temperature range of 300 - 1263 K (12 replicates, 50 nanoseconds). Analogously, the
histogram has one energy minimum populated and the number of times the ~ +90° torsion was observed is fairly narrowly
distributed (Fig. 5, top). With the same initial conformation, increasing the temperature range to a high of 3302 K (20
replicates, 50 nanoseconds), showed some evidence of sampling of the opposite conformation in the radial plot (Fig. 5,
175 middle). Starting the simulation with the 3D conformation switched to put the pendant base towards the back instead and
running 20 replicates for a higher sampling temperature shows both minima were sampled (Fig. 5, bottom). Once this
compound has been synthesized, it then becomes experimentally apparent from the ^1H NMR spectrum at 300 K in DMSO- d_6
that both minima are equally populated (Fig. 2a). In this manner the experimental results can be fed-back to the calculations
to refine details and gauge areas of caution during interpretation.



180

Figure 5. The REST-MD simulation of the dimethyl compound 2 predicts a preference to populate only one energy minimum, correlated with the initial dihedral angle starting condition in the simulation. Shown are results from calculations for conformations sampled as a function of bond rotation angle for the bond between the tricyclic core and the aromatic ring, bolded in the molecular structure. The three different simulation conditions are, from top to bottom: starting with the pendant base facing forward ($\sim +90^\circ$) with a temperature range of 300 - 1263 K (12 replicates); same initial conformation, with a temperature range of 300 - 3302 K (20 replicates); and the opposite initial conformation, with the pendant base facing backward, run with 20 replicates (300 - 3302 K). All REST-MD simulations ran for 50 nanoseconds.

185

2.4 REST-MD/NMR synergy in drug discovery

What REST-MD adds to the existing NMR platform is visualization of conformational dynamics, by providing calculated rotational energy barriers across all bonds. This complements NMR spectral data to give insight into flexibility / rigidity at atomic resolution. Together, REST-MD and NMR conformational analysis allows us to utilize all the spectral information, thermodynamic and kinetic, gathered from ^1H NMR spectra: chemical shifts, J -couplings, NOEs and linewidths, to maximize characterization of free ligands in solution.

Without REST-MD, NMR alone can provide valuable information on the experimental conformational preference of the free ligand in solution. From the NMR alone, the relative populations of each conformer in solution can be deduced. And it can be determined if the dominant conformer in solution is pre-organized into the bioactive conformation, which is of practical value for drug discovery. However, adding REST-MD provides an easy and practical way to visualize the magnitude of the

195

energy penalty paid if the bioactive conformation is not highly populated in solution. This can help rationalize the cost to benefit ratio of ~~effort invested in designing an increase in the percent bioactive conformation by restricting rotation design~~ [team effort invested in increasing the percentage of free ligand pre-organized into a bioactive conformation](#). As drug discovery requires optimization of several parameters, knowing when binding has been optimized can shift design focus and resources towards improving physicochemical properties.

The added benefit of REST-MD is its ability to deliver prospective information regarding structural ideas of compounds, not yet synthesized. Accurate predictions of free ligand solution conformational dynamics can help rank compounds to focus synthesis prioritization and flag supplemental experiments, such as selective NOEs on atom pairs to quickly ascertain expected conformations.

While the full torsional profile is powerful on its own, the REST-MD results also provide an extensively sampled conformational ensemble in explicit solvent that can be clustered and fed forward for use in NMR conformational analysis. Taking the selected conformer set forward for QM geometry refinements and calculations of NMR chemical shift and coupling constants provides the modeled parameter set used for further NAMFIS based analysis. Using the conformer set generated by REST-MD is particularly helpful for higher molecular weight small molecules which begin to self-associate during low mode MD conformational searches ([LaBute, 2010](#)) using a polarizable continuum model to emulate solvent. ~~Low mode MD provides a comprehensive search of the conformational ensemble, but can therefore result in~~ a set highly biased towards collapsed conformations.

215 3 Methods

3.1 NMR Spectroscopy

¹H NMR spectra were recorded at 300 K on a 500 MHz NEO or a 600 MHz AVIII Bruker spectrometer with TCI cryoprobes. Solutions were made from 1-4 mg solid freshly dissolved in DMSO-*d*₆. Spectra were acquired with a 30 degree hard pulse, a 1 sec delay, 2 dummy shots, and signal averaged over 16 transients. A spectral width of ~ 20 ppm with 64k points was used. Spectral analysis was performed using Advanced Chemistry Development, Inc. (ACD/Labs) Spectrum Processor (ACD/Labs, Version 2020.1.2). 2D ROESY was run with the Bruker standard pulse program roesyadsphpr with ns 4, TD (1024, 256), and a 200 ms spin-lock.

3.1.1 Compound 1

¹H NMR (500 MHz, DMSO-*d*₆) Shift 10.54 (s, 1H), 7.44 (d, J = 7.7 Hz, 1H), 7.23 (d, J = 8.0 Hz, 1H), 7.03 (td, J = 7.9, 1.2 Hz, 1H), 6.99 (t, J = 8.2 Hz, 1H), 6.97 (td, J = 8.0, 1.2 Hz, 1H), 6.89 (d, J = 7.9 Hz, 1H), 6.28 (br d, J = 8.2 Hz, 1H), 5.14 (s, 1H), 4.51 (dt, J = 47.5, 6.1 Hz, 2H), 4.00 (t, J = 5.6 Hz, 2H), 3.46 (dq, J = 16.0, 10.6 Hz, 1H), 3.37 – 3.33 (m, 1H), 2.99 (dq, J = 16.0, 10.0 Hz, 1H), 2.90 (t, J = 5.7 Hz, 2H), 2.78 (dd, J = 16.0, 4.5 Hz, 1H), 2.69 (t, J = 6.9 Hz, 2H), 2.62 (dd, J = 16.0, 7.7 Hz, 1H), 2.53 – 2.51 (m, 1H), 2.28 (s, 3H), 1.85 – 1.74 (m, 2H), 1.06 (d, J = 6.7 Hz, 3H)

3.1.2 Compound 2

230 ¹H NMR (500 MHz, DMSO-d₆) Shift 10.18 (s, 0.5H, isomer1), 10.14 (s, 0.5H, isomer2), 7.39 (d, J = 7.6 Hz, 1H, isomer1+isomer2), 7.18 (t, J = 7.2 Hz, 1H, isomer1+isomer2), 7.09 (d, J = 8.5 Hz, 0.5H, isomer2), 6.99 – 6.95 (m, 1H, isomer1+isomer2), 6.95 – 6.90 (m, 1H, isomer1+isomer2), 6.88 (d, J = 8.4 Hz, 0.5H, isomer2), 6.84 (s, 1H, isomer1), 5.38 (s, 0.5H, isomer1), 5.29 (s, 0.5H, isomer2), 4.54 (dt, J = 47.5, 6.0 Hz, 1H, isomer1), 4.44 (dt, J = 47.5, 6.0 Hz, 1H, isomer2), 4.07 – 3.95 (m, 1H, isomer1), 3.95 – 3.85 (m, 1H, isomer2), 3.67 – 3.56 (m, 1H, isomer1+isomer2), 3.39 (s, 1H, isomer1+isomer2), 3.14 – 3.04 (m, 1H, isomer1+isomer2), 2.94 (br t, J = 5.4 Hz, 1H, isomer1), 2.80 (br t, J = 5.6 Hz, 1H, isomer2), 2.77 (br d, J = 4.5 Hz, 1H, isomer1+isomer2), 2.72 (t, J = 7.0 Hz, 1H, isomer1), 2.69 (br d, J = 15.0 Hz, 1H, isomer1+isomer2), 2.60 (t, J = 6.9 Hz, 1H, isomer1+isomer2), 2.44 (s, 1.5H, isomer2), 2.39 (s, 1.5H, isomer2), 1.83 (br dquin, J = 26.2, 6.6 Hz, 1H, isomer1), 1.82 (s, 1.5H, isomer2), 1.80 (s, 1.5H, isomer1), 1.72 (dquin, J = 26.2, 6.4 Hz, 1H, isomer2), 1.14 (d, J = 6.5 Hz, 3H, isomer1+isomer2)

240 3.1.3 Compound 3

¹H NMR (600 MHz, DMSO-d₆) Shift 10.86 (s, 1H), 7.45 (d, J = 7.8 Hz, 1H), 7.31 (d, J = 8.0 Hz, 1H), 7.26 (t, J = 7.8 Hz, 1H), 7.08 (dd, J = 8.0, 7.5 Hz, 1H), 7.00 (dd, J = 7.8, 7.5 Hz, 1H), 6.86 (dd, J = 8.2, 2.4 Hz, 1H), 6.84 (d, J = 7.8 Hz, 1H), 6.75 (br d, J = 2.3 Hz, 1H), 4.98 (s, 1H), 4.48 (dt, J = 47.5, 6.6 Hz, 2H), 3.95 (t, J = 5.6 Hz, 2H), 3.57 (qd, J = 13.0, 9.3 Hz, 1H), 3.12 (dq, J = 11.0, 6.8, 5.0 Hz, 1H), 3.01 (qd, J = 18.0, 9.3 Hz, 1H), 2.83 (t, J = 5.7 Hz, 2H), 2.64 (dd, J = 15.8, 5.0 Hz, 1H), 2.57 (dd, J = 15.8, 11.0 Hz, 1H), 2.62 (t, J = 6.6 Hz, 2H), 1.76 (dquin, J = 26.1, 6.6 Hz, 2H), 1.11 (d, J = 6.8 Hz, 3H)

3.2 Exchange Spectroscopy

¹H NMR spectra were recorded on a 500 MHz NEO at 300, 305, 310, 340, 345, 350, 355, 360, 365, and 373 K. For the 1D selective exchange spectroscopy at 300, 300, and 310 K, the mixing times used were 100, 200, 300, 400, 500, 700, 1000, and 2000 milliseconds. The spectra were integrated with consistent integral ranges and calibrating the integral of the inverted peak to 100 to consistently normalize the data (Hu and Krishnamurthy, 2006). An excel spreadsheet was used to calculate the fractional intensity increase as a function of mixing time to fit exchange rate and half-life (Bovey, 1988; Li, et al., 2007).

3.3 REST-MD

Two different initial molecular conformations were run where the variation was placed on the relative position of the pendant base to the tricyclic ring: (i) "forward" or (ii) "backward", using the same atom numbering for all conformations sampled for the same compound, to simplify later steps in the workflow. Molecular protonation states at pH 7.0 ± 0.0 were used for the MD simulations. The force field builder in Maestro (Schrödinger, 2020b) was used to customize the OPLS3e force field for the system builder where a NaCl salt concentration of 0.15 M was used and the base was neutralized by addition of 1 Na⁺ ion during creation of the explicit water shell for solvation using the predefined SPC model and an orthorhombic box shape

of 10 Å x 10 Å x 10 Å using the "buffer" box size calculation method. Desmond (Schrödinger, 2020a) replica exchange with
260 solute tempering molecular dynamics was run with 12 replicas giving a temperature range of 300 K to typically ~1300 K, for
a total of 50 ns for extensive sampling of conformational space during the simulation.

3.4 Simulation Interaction Diagram

The plots automatically generated in Maestro (Schrödinger, 2020b) provide solid lines tracing out the barrier to rotation in
kcal/mol as a function of the torsion angle. The histograms provide the resulting distribution of 1002 conformers under our
265 routine sampling conditions. Radial plots show the evolution of the simulation time from the start, at the center.

3.5 Clustering of Conformers

Ligands, without the solvent shell, were extracted from the REST-MD trajectories for both sets of initial conformers
(forward and backward). To aid a quick visual inspection of the results, conformers were superimposed using the SMARTS
method and the substructure smiles string of c12c(C)c(CN)[nH]c1cccc2 to align the conformers relative to the rigid tricyclic
270 ring. Conformers were clustered in Maestro (Schrödinger, 2020b) by atomic RMSD, discarding mirror-image conformers,
selecting the option of one structure (nearest to centroid) per cluster, thus reducing the full set down to representative diverse
conformers, typically 15 - 40.

3.6 QM Calculations

Chemical Computing Group's (Molecular Operating Environment (MOE), 2019.01) conformational search GUI was
275 employed to generate input files for Gaussian 16 (Revision C.01) after importing conformers into a molecular database and
using the wash function to neutralize charged species not observed by NMR in DMSO-*d*₆ solutions. QM geometry
refinement, chemical shift calculations and coupling constant calculations were carried out with the GIAO DFT method at
the B3LYP/6-31G* level with PCM solvent modeling using a dielectric constant of 78.4. Geometry optimization keywords
were set with `opt=(tight,RecalcFC=5,MaxCycles=5000)` and `Int=SuperFineGrid`.

280 3.7 Conformer Distribution

MOE's Spectral Analysis GUI was employed for least squares fits of chemical shifts to determine conformer distributions;
the option for couplings and NOE's was used selectively.

4 Conclusions

The REST-MD protocols described above provide rapid and prospective access to torsional energy barriers and
285 conformational states for drug-like molecules. The REST-MD calculations accurately reproduce and visualize NMR
dynamics which synergistically work with experimental conformational exchange dynamics obtained from 1D ¹H NMR

spectra. Integration of REST-MD into our NMR conformational analysis platform has enabled visualization of atomic level information by all medicinal chemists and can be readily used to guide design hypotheses toward molecules with improved potency and or physicochemical properties.

290 This new methodology has been applied across more than 10 early oncology projects in 2020, both small molecules and PROTACs, to answer questions around conformational preference (populations) and dynamics (rotational barriers).

In addition, NMR provides design teams with information on the presence of intramolecular hydrogen bonds (IMHB), and the combined influences on properties such as potency, permeability and oral bioavailability. Diverse applications have enabled refinement of the approach, and represents a step towards the goal of routine use for prospective design and

295 determination of experimentally based conformation-activity relationships.

Author contribution

AB and EC drove the earliest drafts of this manuscript, to which all authors have contributed. MP developed and optimized computational workflows. DL and ND determined the energy barrier to rotation by NMR. AB ran REST-MD simulations in Schrödinger and NAMFIS-based analyses in MOE. All authors contributed valuable discussions to the preparation of this

300 manuscript.

Competing interests

All authors are shareholders in AstraZeneca PLC.

Acknowledgements

The entire SERD team, including the analytical, computational, synthetic, and lead chemists, from the extended Oncology
305 R&D group are gratefully acknowledged for chemical designs, syntheses, purifications and compound profiling. We thank Jason Breed for the crystallography providing protein-ligand and bound conformations shown in Figure 1. An excel spreadsheet with detailed methodology for the 1D selective EXSY was kindly provided by David Whittaker. We thank Jamie Scott and Michelle Lamb for valuable feedback on the manuscript.

References

310 ACD/ChemSketch, version 2020.1.2, Advanced Chemistry Development, Inc., Toronto, ON, Canada, <http://www.acdlabs.com>, 2021.

- Atilaw, Y., Poongavanam, V., Nilsson, C. S., Nguyen, D., Giese, A., Meibom, D., Erdelyi, M., and Kihlberg, J.: Solution Conformations Shed Light on PROTAC Cell Permeability, *ACS Med. Chem. Lett.*, 12, 107-114, <https://doi.org/10.1021/acsmchemlett.0c00556>, 2021.
- 315
- Balazs, A. Y. S., Carbajo, R. J., Davies, N. L., Dong, Y., Hird, A. W., Johannes, J. W., Lamb, M. L., McCoull, W., Raubo, P., Robb, G. R., Packer, M. J., and Chiarparin, E.: Free Ligand 1D NMR Conformational Signatures To Enhance Structure Based Drug Design of a Mcl-1 Inhibitor (AZD5991) and Other Synthetic Macrocycles, *Journal of medicinal chemistry*, 62, 9418-9437, doi:10.1021/acs.jmedchem.9b00716, 2019.
- 320
- Blundell, C. D., Nowak, T., and Watson, M. J.: Measurement, Interpretation and Use of Free Ligand Solution Conformations in Drug Discovery, *Progr. Med. Chem.*, 55, 45-147, <https://doi.org/10.1016/bs.pmch.2015.10.003>, 2016.
- 325
- Blundell, C., Packer, M., and Almond, A.: Quantification of free ligand conformational preferences by NMR and their relationship to the bioactive conformation, *Bioorganic & medicinal chemistry*, 21, 4976-4987, doi:10.1016/j.bmc.2013.06.056, 2013.
- Bovey, F. A.: *Nuclear Magnetic Resonance Spectroscopy*, Second Edition, Academic Press, Inc., San Diego, California, pp. 291-299, <https://doi.org/10.1016/B978-0-08-091699-6.50010-6>, 1988.
- 330
- Chiarparin, E., Packer, M. J., and Wilson, D. M.: Experimental free ligand conformations: a missing link in structure-based drug discovery, *Future Med. Chem.*, 11, 79-82, <https://doi.org/10.4155/fmc-2018-0339>, 2019.
- 335
- Cicero, D., Barbato, G., and Bazzo, R.: NMR Analysis of Molecular Flexibility in Solution: A New Method for the Study of Complex Distributions of Rapidly Exchanging Conformations. Application to a 13-Residue Peptide with an 8-Residue Loop, *J. Am. Chem. Soc.*, 117, 1027-1033, <https://doi.org/10.1021/ja00108a019>, 1995.
- de Sena M Pinheiro, P., Rodrigues, D. A., do Couto Maia, R., Thota, S., and Fraga, C.: The Use of Conformational Restriction in Medicinal Chemistry, *Curr. Top. Med. Chem.*, 19, 1712-1733, <https://doi.org/10.2174/1568026619666190712205025>, 2019.
- 340
- Fang, Z., Song, Y., Zhan, P., Zhang, Q., and Liu, X.: Conformational restriction: an effective tactic in 'follow-on'-based drug discovery, *Future Med. Chem.*, 6, 885-901, <https://doi.org/10.4155/fmc.14.50>, 2014.
- 345

Farès, C., Lingnau, J. B., Wirtz, C., and Sternberg, U., Conformational Investigations in Flexible Molecules Using Orientational NMR Constraints in Combination with 3J -Couplings and NOE Distances. *Molecules*, 24, 4417-4441. <https://doi.org/10.3390/molecules24234417>, 2019.

350 Foloppe, N. and Chen, I.-J.: Towards understanding the unbound state of drug compounds: Implications for the intramolecular reorganization energy upon binding, *Bioorgan. Med. Chem.*, 24, 2159-2189, <https://doi.org/10.1016/j.bmc.2016.03.022>, 2016.

355 Gaussian 16, Revision C.01, Frisch, M. J., Trucks, G. W., Schlegel, H. B., Scuseria, G. E., Robb, M. A., Cheeseman, J. R., Scalmani, G., Barone, V., Petersson, G. A., Nakatsuji, H., Li, X., Caricato, M., Marenich, A. V., Bloino, J., Janesko, B. G., Gomperts, R., Mennucci, B., Hratchian, H. P., Ortiz, J. V., Izmaylov, A. F., Sonnenberg, J. L., Williams-Young, D., Ding, F., Lipparini, F., Egidi, F., Goings, J., Peng, B., Petrone, A., Henderson, T., Ranasinghe, D., Zakrzewski, V. G., Gao, J., Rega, N., Zheng, G., Liang, W., Hada, M., Ehara, M., Toyota, K., Fukuda, R., Hasegawa, J., Ishida, M., Nakajima, T., Honda, Y., Kitao, O., Nakai, H., Vreven, T., Throssell, K., Montgomery, J. A., Jr., Peralta, J. E., Ogliaro, F., Bearpark, M. J., 360 Heyd, J. J., Brothers, E. N., Kudin, K. N., Staroverov, V. N., Keith, T. A., Kobayashi, R., Normand, J., Raghavachari, K., Rendell, A. P., Burant, J. C., Iyengar, S. S., Tomasi, J., Cossi, M., Millam, J. M., Klene, M., Adamo, C., Cammi, R., Ochterski, J. W., Martin, R. L., Morokuma, K., Farkas, O., Foresman, J. B., Fox, D. J. Gaussian, Inc., Wallingford CT, 2016

Hu, H. and Krishnamurthy, K.: Revisiting the initial rate approximation in kinetic NOE measurements, *J. Magn. Reson.*, 365 182, 173-177, <https://doi.org/10.1016/j.jmr.2006.06.009>, 2006.

Huang, X., Hagen, M., Kim, B., Friesner, R. A., Zhou, R., and Berne, B. J.: Replica exchange with solute tempering: efficiency in large scale systems, *J. Phys. Chem. B*, 111, 5405-5410, <https://doi.org/10.1021/jp068826w>, 2007.

370 [Labute, P.: LowModeMD-Implicit Low-Mode Velocity Filtering Applied to Conformational Search of Macrocycles and Protein Loops. *J. Chem. Inf. Model.*, 50, 792-800, https://doi.org/10.1021/ci900508k, 2010.](https://doi.org/10.1021/ci900508k)

LaPlante, S. R., Edwards, P. J., Fader, L., Jakalian, A., and Hucke, O.: Revealing atropisomer axial chirality in drug discovery, *ChemMedChem*, 6, 505-513 <https://doi.org/10.1002/cmdc.201000485>, 2011a.

375 LaPlante, S. R., Fader, L. D., Fandrick, K. R., Fandrick, D. R., Hucke, O., Kemper, R., Miller, S. P. F., and Edwards, P. J.: Assessing atropisomer axial chirality in drug discovery and development, *J. Med. Chem.*, 54, 7005-7022, <https://doi.org/10.1021/jm200584g>, 2011b.

380 LaPlante, S. R., Nar, H., Lemke, C. T., Jakalian, A., Aubry, N., and Kawai, S. H.: Ligand bioactive conformation plays a
critical role in the design of drugs that target the hepatitis C virus NS3 protease, *J. Med. Chem.*, 57, 1777-1789,
<https://doi.org/10.1021/jm401338c>, 2014.

Li, F., Zhang, H., Jiang, L., Zhang, W., Nie, J., Feng, Y., Yang, M., and Liu, M.: Dynamic NMR study and theoretical
385 calculations on the conformational exchange of valsartan and related compounds, *Magn. Reson. Chem.*, 45, 929-936,
<https://doi.org/10.1002/mrc.2072>, 2007.

Liu, P., Kim, B., Friesner, R A., and Berne, B. J.: Replica exchange with solute tempering: a method for sampling biological
systems in explicit water, *P. Natl. Acad. Sci. USA*, 102, 13749-13754, <https://doi.org/10.1073/pnas.0506346102>, 2005.

390 Molecular Operating Environment (MOE), 2019.01, Chemical Computing Group ULC, 1010 Sherbooke St. West, Suite
#910, Montreal, QC, Canada, H3A 2R7, 2021.

Nevins, N., Cicero, D., and Snyder, J. P.: A Test of the Single-Conformation Hypothesis in the Analysis of NMR Data for
395 Small Polar Molecules: A Force Field Comparison, *J. Org. Chem.*, 64, 3979-3986, <https://doi.org/10.1021/jo9824450>, 1999.

Schrödinger Release 2020-3: Desmond Molecular Dynamics System, D. E. Shaw Research, New York, NY, 2020. Maestro-
Desmond Interoperability Tools, Schrödinger, New York, NY, <https://www.schrodinger.com/products/desmond>, 2020a.

400 Schrödinger Release 2020-3: Maestro, Schrödinger, LLC, New York, NY, <https://www.schrodinger.com/products/maestro>,
2020b.

Scott, J. S., Bailey, A., Davies, R. D., Degorce, S. L., MacFaul, P. A., Gingell, H., Moss, T., Norman, R. A., Pink, J. H.,
Rabow, A. A., Roberts, B., and Smith, P. D.: Tetrahydroisoquinoline Phenols: Selective Estrogen Receptor Downregulator
405 Antagonists with Oral Bioavailability in Rat, *ACS Med. Chem. Lett.*, 7, 94-99,
<https://doi.org/10.1021/acsmedchemlett.5b00413>, 2016.

Scott, J. S., Bailey, A., Buttar, D., Carbajo, R. J., Curwen, J., Davey, P. R. J., Davies, R. D. M., Degorce, S. L., Donald, C.,
Gangl, E., Greenwood, R., Groombridge, S. D., Johnson, T., Lamont, S., Lawson, M., Lister, A., Morrow, C. J., Moss, T. A.,
410 Pink, J. H., and Polanski, R.: Tricyclic Indazoles-A Novel Class of Selective Estrogen Receptor Degradation Antagonists, *J.*
Med. Chem., 62, 1593-1608, <https://doi.org/10.1021/acs.jmedchem.8b01837>, 2019.

415 Scott, J. S., Moss, T. A., Balazs, A., Barlaam, B., Breed, J., Carbajo, R. J., Chiarparin, E., Davey, P. R. J., Delpuech, O.,
Fawell, S., Fisher, D. I., Gargica, S., Gangl, E. T., Grebe, T., Greenwood, R. D., Hande, S., Hatoum-Mokdad, H., Herlihy,
K., Hughes, S., Hunt, T. A., Huynh, H., Janbon, S. L. M., Johnson, T., Kavanagh, S., Klinowska, T., Lawson, M., Lister, A.
S., Marden, S., McGinnity, D. F., Morrow, C. J., Nissink J. W. M., O'Donovan, D. H., Peng, B., Polanski, R., Stead, D. S.,
Stokes, S., Thakur, K., Throner, S.R., Tucker, M. J., Varnes, J., Wang, H., Wilson, D. M., Wu, D., Wu, Y., Yang, B., and
Yang, W.: Discovery of AZD9833, a Potent and Orally Bioavailable Selective Estrogen Receptor Degradar and Antagonist,
63, 14530-14559, *J. Med. Chem.*, <https://doi.org/10.1021/acs.jmedchem.0c01163>, 2020.

420

Slabber, C. A., Grimmer, C. D., and Robinson, R. S.: Solution Conformations of Curcumin in DMSO, *J. Nat. Prod.*, 79,
2726-2730, <https://doi.org/10.1021/acs.jnatprod.6b00726>, 2016.

425 Wang, L., Friesner, R. A., and Berne, B. J.: Replica exchange with solute scaling: a more efficient version of replica
exchange with solute tempering (REST2), *J. Phys. Chem. B*, 115, 9431-9438, <https://doi.org/10.1021/jp204407d>, 2011.

430 Wipf, P., Skoda, E. M., and Mann, A.: Conformational Restriction and Steric Hindrance in Medicinal Chemistry, in: *The
Practice of Medicinal Chemistry*, Fourth edition, edited by: Wermuth, C. G., Aldous, D., Raboisson, P., and Rognan, D.,
Academic Press, San Diego, 279 - 299, <https://doi.org/10.1016/B978-0-12-417205-0.00011-0>, 2015.

Wu, J., Lorenzo, P., Zhong, S., Ali, M., Butts, C. P., Myers, E. L., and Aggarwal, V. K.: Synergy of synthesis, computation
and NMR reveals correct baulamycin structures, *Nature*, 547, <https://doi.org/10.1038/nature23265>, 2017.

Zondlo, N. J.: SAR by 1D NMR, *J. Med. Chem.*, 62, 9415-9417, <https://doi.org/10.1021/acs.jmedchem.9b01688>, 2019.